

A Review of Research on Grove Mountains CM-Type Chondrites

Wenjie Shen ^{1,2,3,4,*}, Zhipeng Liang ¹, Tianxiang Zou ¹, Zhijun Yang ^{1,2}, Weisheng Hou ^{1,2} , Meng Zhou ¹ and Jialin Gong ¹

- ¹ School of Earth Sciences and Engineering, Sun Yat-sen University, Zhuhai 519000, China; liangzhp9@mail2.sysu.edu.cn (Z.L.); zoutx@mail2.sysu.edu.cn (T.Z.); yangzhj@mail.sysu.edu.cn (Z.Y.); houwsh@mail.sysu.edu.cn (W.H.); zhous47@mail2.sysu.edu.cn (M.Z.); gongjlin@mail2.sysu.edu.cn (J.G.)
- ² Guangdong Key Laboratory of Geological Process and Mineral Resources Exploration, Zhuhai 519000, China
- ³ Guangdong Provincial Key Laboratory of Geodynamics and Geohazards, Zhuhai 519000, China
- ⁴ Earth Resources and Earth Environment Research Center, Sun Yat-sen University, Zhuhai 519000, China
- * Correspondence: shenwjie@mail.sysu.edu.cn

Abstract: CM chondrite is the most important carbonaceous chondrite containing abundant Ca, Al-rich inclusions (CAIs) and other interesting objects, which probably experienced early condensation processes in the Solar Nebula environment and later alteration in parent body surroundings. Thus, it is a vital raw material to explore in the formation and evolution of the early Solar System. Grove Mountains (GRV) CM chondrites have been collected from Antarctica by Chinese Antarctic Research Expedition (CARE) for nearly 20 years. In this paper, we review the study of GRV CM chondrites. In total, there are eight CM chondrites named Grove Mountains officially approved by the Meteoritical Society. Petrology and mineral, matrix, CAIs, metal and sulfide in GRV CM chondrites are carefully reviewed. All the meteorites have similar characteristics with a dominant component of matrix. Phyllosilicate minerals generally developed in the matrix. The different altered mineral assemblages, contents and chemical compositions show that these chondrites underwent varying degrees of aqueous alteration, of which GRV 020005 is the most heavily altered CM chondrite. GRV 020025 is the second heaviest of the CM samples with the most extensive studies among these chondrites. It contains abundant CAIs and amoeboid olivine aggregates (AOAs). The modal content is about 1.0 vol% for CAIs. The findings of some new types of CAIs (such as hibonite-rich and spinel-pyroxene inclusions with forsterite-rich accretionary rims), AOAs and a complex, fine-grained P-bearing sulfide phase enrich the study of GRV 020025.

Keywords: CM chondrite; Grove Mountains; CAIs; GRV 020025



Citation: Shen, W.; Liang, Z.; Zou, T.; Yang, Z.; Hou, W.; Zhou, M.; Gong, J. A Review of Research on Grove Mountains CM-Type Chondrites. *Minerals* **2022**, *12*, 619. <https://doi.org/10.3390/min12050619>

Academic Editors: Guiqin Wang, Yang Liu and Jesus Martinez-Frias

Received: 24 March 2022

Accepted: 9 May 2022

Published: 13 May 2022

Publisher's Note: MDPI stays neutral with regard to jurisdictional claims in published maps and institutional affiliations.



Copyright: © 2022 by the authors. Licensee MDPI, Basel, Switzerland. This article is an open access article distributed under the terms and conditions of the Creative Commons Attribution (CC BY) license (<https://creativecommons.org/licenses/by/4.0/>).

1. Introduction

Carbonaceous chondrites (CCs) are fragments of hydrated asteroids and among the oldest and most primitive objects that provide insights into the early protoplanetary disk, the formation of the planets and the origin of water and life [1–3]. The major chemical groups of CCs include the Ivuna-type (CI), Mighei-type (CM), Ornans-type (CO), Vigarano-type (CV), Karoonda-type (CK), Renazzo-type (CR), Bencubbin-type (CB), ALH 85085-type (CH) and Loongana-type (CL) [4,5]. The CM chondrites are of particular interest, as they are the most abundance group of CCs and are the material most frequently found as clasts within other types of meteorites [6,7]. This suggests that the CM parent asteroids are (or were) widespread in the asteroid belt, including the regions providing samples to Earth [8]. Up to date (1 February 2022), there are 715 pieces of CM chondrites according to Meteoritical Bulletin Database [9], accounting for about 25% of the total CCs and approximately 0.9% of all the officially named meteorites.

Antarctica is a cold and dry continent covered with ice and snow. Thus, it is a wonderful place to preserve and collect meteorites. Now, there are 1339 pieces of CCs found by Antarctic scientific expedition teams sent by various countries that occupied 47%

of the total CCs. The proportion of CM chondrites is the highest, which is much higher than other types of CCs, reaching about 42% (564 pieces) out of the total Antarctic CCs. Thus, Antarctica is the most important enrichment site of CM-type meteorites.

In the last years, Grove Mountains was selected as an area of high meteorite concentration in Antarctica. Since the first expedition in 1998, 12,665 pieces of meteorites have been collected by CARE in this region and China has been one of the biggest owners of Antarctic meteorites [10]. Many special types of meteorites have been found, such as Martian meteorites, Vesta meteorites, enstatite chondrites, eucrites, acapulcoites, winonaites, pallasites and so on. Comparing with the 2.8% recovery rate in the Antarctic continent, the CCs recovery rate in Grove Mountains is only 0.37%. There are 21 CCs found in Grove Mountains, of which 8 are CM chondrites. In this paper, we review and summarize the study of GRV CM chondrites in Antarctica and provide some new directions for further research on GRV CM chondrites.

2. Sample Description

The CM chondrite samples include GRV 020005, GRV 020017, GRV 020025, GRV 021536, GRV 021580, GRV 050179, GRV 050384 and GRV 13051 collected from Grove Mountains, Antarctica. Among these samples, GRV 020025 is the most intensively studied by several researchers (Table 1). All these samples are relatively small in weight with mass ranging from 0.4 to 5 g. The samples are black irregular fragments. They are relatively fresh. Some of them are almost completely covered by black fusion crust (Figure 1C,D) and others are only partially covered (Figure 1A,B).

Table 1. General information of CM chondrites found in Grove Mountains, Antarctica.

Number	Name	Status	Fall	Year	Type	Mass (g)	MetBul	Works
1	GRV 020005	Official	N	2002	CM2	0.4	89	[11]
2	GRV 020017	Official	N	2002	CM2	2.2	89	[11–13]
3	GRV 020025	Official	N	2002	CM2	3.55	89	[11–16]
4	GRV 021536	Official	N	2003	CM2	1.45	93	[17]
5	GRV 021580	Official	N	2003	CM2	0.48	96	
6	GRV 050179	Official	N	2006	CM2	5.03	93	[18]
7	GRV 050384	Official	N	2006	CM2	0.76	95	
8	GRV 13051	Official	N	2014	CM2	3.47	103	

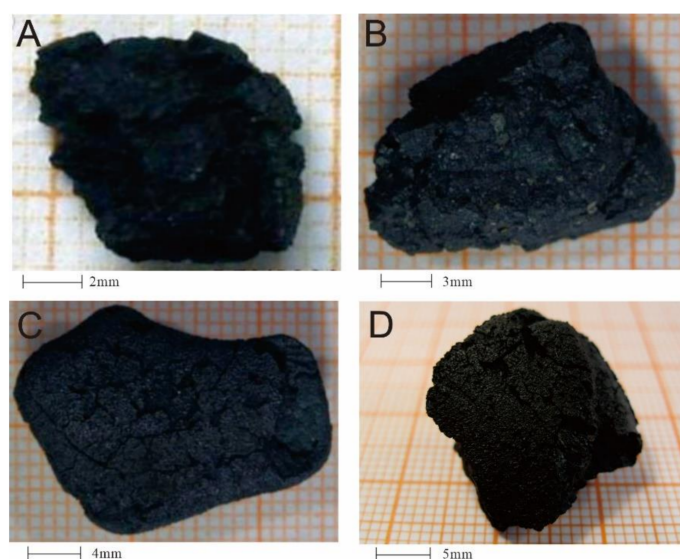


Figure 1. Typical specimens of CM chondrites in Grove Mountains, Antarctica: (A) GRV 020005; (B) GRV 020017; (C) GRV 020025; (D) GRV 050179.

3. Petrology and Mineralogy

3.1. General Description

In these GRV CM chondrites, four samples (GRV 020005, GRV 020017, GRV 020025 and GRV 050179) were studied in relative detail (Tables 1 and 2). Dai [14] first investigated the thin sections of GRV 020017 and GRV 020025. Several years later, Wang [15] observed new slices of these samples. In general, the GRV CM chondrites show similar petrographic properties of average CM chondrites [19] in chondrule/matrix abundance and size distribution (Table 2). The relative low CAI and AOA and high sulfide abundance probably resulted from the heterogeneous sampling on parent body and (or) selective alteration. Statistical error may sometimes be a possible factor leading to different results, especially in measuring the low content indicators (such as sulfide, metal and CAIs, Table 2). According to the published data by Shen et al. [20], GRV 020025 has a CAI content of up to 1.0%, which is much close to the average value of the CM chondrites (1.2%). The sample of GRV 020005 is quite different from other samples in chondrule size and content (low) and matrix content (high) which just shows the CM1 petrologic type [15].

Table 2. Summary of average petrographic properties of the GRV CM chondrites.

Name	Type	Chd	Chd Dia	CAIs	Matrix	Sulfide/Metal	Matrix/Chd
GRV 020005	CM1	14 *	0.2 (0.1–0.6) *	-	83 *, 86 **	~3.0/0 *	6.0 *
GRV 020017	CM2	30–40 [§] , 20 *, 25 &	0.05–0.3 [§] , 0.3 (0.1–1.3) *	0.1 [§]	60–70 [§] , 80 *, 81 **, 70 &	1.8 [§] , 5.0/0.1 *, 1 &	2.0 [§] , 4.0 *, 2.8 &
GRV 020025	CM2	26 [§] , 20 *, 25 &	0.1–0.3 [§] , 0.3 (0.1–1.0) *	0.29 [§] , 1.0 #	72 [§] , 79 *, 80 **, 70 &	1.4 [§] , 1.0/0.1 *, 0.1 &	2.8 [§] , 4.0 *, 2.8 &
GRV 050179 ^{§§}	CM2	25	most <0.5 (0.35–0.6);	0.29	74	1.5/0.4	3.0
GRV 021579	CO3/CM2?	45 [§] , 22 *	0.03–0.1 [§] ; 0.2 (0.1–0.8) *	0.81 [§]	54 [§] , 76 *, 78 **	0.4 [§] , 2 *, 2 &	1.2
Average CM ^{##}	-	20	0.3	1.2	70	0.1	3.5

*: data from [11]; **: data acquired by backscatter image from [11]; [§]: data from [12]; #: data from [20]; ^{§§}: data from [18]; ^{##}: data from [19]; &: data from [13]. Chd: chondrule; Chd Dia: chondrule diameter; CAIs: calcium, aluminum-rich inclusions.

The petrological and mineralogical characteristics of GRV 020017 and GRV 020025 are similar, mainly composed of opaque matrix and a small amount of high-temperature components (including chondrule, CAIs and crystal clast) with fine-grained rims. Electron microprobe analysis on olivine and pyroxene in the chondrule and matrix of GRV 020017 and GRV 020025 shows that they have similar mineral composition patterns. The values of olivine Fa, low-Ca pyroxene Fs, En and Wo are summed up in Table 3. The chemical composition of olivine and pyroxene is very heterogeneous as indicated by the high PMD value (>>5, Table 3) [11–13,16]. It is noteworthy that the chemical composition of olivine in the chondrules of GRV 020025 is relatively uniform (Fa: 0.8–1.1 with one exception of 4.7) [12] while it varies largely in the olivine clasts (Fa: 0.6–48.3) [13].

Table 3. Mineral composition of olivine and pyroxene in GRV 020017 and GRV 020025.

Samples	GRV 020017			GRV 020025		
Reference	[11] *	[12]	[13]	[11] *	[12]	[13]
Fa	27 (1.0–44.3)	12 (0.2–94)	0.24–34.4	28 (1.2–68.6)	9 (0.7–48.3)	0.57–48.3
PMD	58	163	145	87	158	173
Fs	3.6 (1.6–4.6)	2.8 (0.4–14)	0.57–13.6	11 (4.3–14.5)	3.8 (0.6–16.4)	0.68–4.76
PMD	32	128	169	53	150	63
En	91.4–95.6		60–98.6	76.2–94.6		93.8–97.7
Wo	0.6–4.6		0.73–4.19	1.2–9.3		0.45–4.67

*: data of matrix olivine and pyroxene. Fa: fayalite. PMD: percent mean deviations. Fs: ferrosilite. En: enstatite. Wo: wollastonite.

3.2. Matrix

Matrix material is best defined as the optically opaque mixture of mineral grains 10 nm to 5 mm in size distinguishing from fragments of chondrules, CAIs and other

components by their distinctive sizes, shapes and textures [19]. So far, Professor Miao Bingkui's team [11,13] has carefully studied the matrix of three GRV CM chondrites (GRV 02005, GRV 020017 and GRV 020025). The matrix is mainly divided into three types of interstitial matrix, fine-grained rim (FGR) and dark inclusions (DIs).

3.2.1. Texture and Mineralogy

Interstitial matrix is the major form existing in the three GRV CM chondrites, which is mainly composed of tochilinite-cronstedtite intergrowths (TCIs, formerly referred to in the literature as “poorly characterized phases” or PCPs) [21,22]. The TCI proportion is about 50 vol%, 35 vol% and 28 vol% in GRV 02005, GRV 020017 and GRV 020025, respectively. FGR typically accounts for 4.3 vol%, 20.9 vol% and 22.7 vol% in these CM chondrites and there is a weak (GRV 020005) to significant (GRV 020017 and GRV 020025) positive correlation between FGR thickness and internal chondrule (and CAI) diameter. There are 9 DIs found in GRV CM chondrite matrices and most DIs are type B inclusions. Matrices of these three CM chondrules predominantly contain similar mineral compositions such as phyllosilicate (largely serpentines with diverse morphologies, degrees of crystallinity and compositions), magnetite, sulfide and carbonate (calcite and/or dolomite). Anhydrous silicate mineral (olivine and pyroxene) does not appear in GRV 020005, but in GRV 020017 and GRV 020025. Dolomite is commonly found in the matrix carbonate (~30%) of GRV 020005, but no dolomite in GRV 020017 and GRV 020025, which shows their varying degrees of aqueous alteration. Fe-Ni metal (kamacite) is present as grains of 50–200 nm size in the matrix of GRV 020017 and GRV 020025, but not found in the GRV 020005. Sulfide mainly includes pentlandite and pyrrhotite, followed by mesophase (mainly in GRV 020025) and troilite (mainly in GRV 020017 and GRV 020025) scattering in the matrix with grain size of 1–20 μm . In addition, P-bearing sulfide phase (also named as P-O-rich sulfide) is present in GRV 021536 and occurred mainly as isolated fragments or aggregates with irregular fractures in the matrix [17]. No other occurrence of P-bearing sulfide was observed in this chondrite.

3.2.2. Mineral and Whole Rock Geochemistry

Matrix olivine, pyroxene, sulfide, metal, carbonate phyllosilicate and whole rock composition were analyzed using electron probe microanalyzer (EPMA) [11]. The mean Fa value of matrix olivine is 27 (1.0–44.3) and 28 (1.2–68.6) with high PMD of 58 and 87 for GRV 020027 and GRV 020025, respectively (Table 3). Olivine FeO and MnO show obvious positive correlation when the Fa value is up to 10. Pyroxene is mainly low calcium pyroxene (orthopyroxene) and its composition is relatively uniform compared with olivine (Table 3, with relative low PMD of 32 and 58 in pyroxene for GRV 020027 and GRV 020025, respectively). In GRV 020025, high calcium pyroxene (clinopyroxene) is also present (Fs: 16.1–18.0, En: 56.3–55.5; Wo: 26.5–27.6). Al_2O_3 is positive correlation with TiO_2 both in low calcium pyroxene and in high calcium pyroxene.

Two grains of kamacite analyses indicate that the composition of Fe, Ni, Co and P is 93.5%, 5.82%, 0.39% and 0.24% and 94.6%, 6.01%, 0.72%, 0.28% in GRV 020017 and GRV 020025, respectively. It shows that the Co/Ni ratios of GRV 020017 and GRV 020025 are 0.94 and 0.95 respectively, while the Fe/(Fe + Ni) ratios are 0.07 and 0.08 respectively. The decreasing order of these samples arranged by Ni content in pentlandite is GRV 020005 (32.53%), GRV 020025 (32.18%) and GRV 020017 (27.62%).

The compositions of calcite in the matrix of three samples are relatively similar and they all contain a certain amount of FeO (0.91–1.54%), MnO (0.31–0.72%) and MgO (0.10–0.26%), although the contents of FeO (4.91% in average) and NiO (21.7% in average) are relatively high in some GRV 020025 calcite grains. The average Mg content of matrix dolomite in GRV 020005 is 14.8%, and the Ca content is 28.5%. In addition, it also contains high FeO (4.40%) and MnO (4.59%).

The coarse-grained phyllosilicate (TCI/PCP) is irregular and bright in the BSE image. Electron microprobe analysis on phyllosilicate showed that the total oxides in three GRV

chondrite matrices was low (ranging from 80 to 86%). The composition triangle diagram of Si-Mg-Fe shows that the phyllosilicate is mainly composed of serpentine and cronstedtite.

The matrix whole rock composition was measured by EPMA, using defocus method with beam spot diameter of 10 μm . The results show that the total oxides are less than 90% in all three chondrites due to the existence of volatile matter (such as carbon and water) and microcracks. On the Fe-Mg-Si + Al triangle diagram, the spots of GRV 020005 fall strictly on the serpentine line, which reveals more Mg content in the GRV 020025 matrix than other meteorites. The GRV 020017 spots are relatively scattered, but they all fall near the serpentine line. The spots of GRV 020025 are much scattered, within the range of serpentine and cronstedtite. According to the whole rock composition, the content of S is positively correlated to Ni and Fe is negatively correlated to Si. The ratio of Ca/Al is 0.2, 0.3 and 0.5 in the matrix of GRV 020005, GRV 020025 and GRV 020017, respectively.

3.3. CAIs

CAIs were found in almost all GRV CM chondrites when they were reported to the International Society for Meteoritics and Planetary Science [9]. However, in-depth researches on CAIs (petrology and mineral chemistry) were only carried out in the samples of GRV 020025 and GRV 050179 [12,14–16,18,20].

3.3.1. GRV 020025

A total of 11 CAIs (including 6 type-A-like inclusions, 4 spinel-pyroxene inclusions and one spinel spherule, Figure 2A–C) were identified giving a modal abundance of 0.29 vol% [12,14]. Except for spinel spherule, all other CAIs had undergone varying degrees of aqueous alteration, which transformed melilite into phyllosilicate, especially in type-A-like inclusions. FGRs around the inclusions are commonly present and they are usually layered with the inner most layer rich in FeO. Later, the same section of GRV 020025 were carefully observed and 20 new CAIs and 6 AOAs were identified, with yield being a total modal abundance of 1.0 vol% for CAIs [20]. Although there is no more information on these inclusions after that, it is certain that they are new types of CAIs such as hibonite-rich inclusions and forsterite-rich accretionary rims.

Type-A like inclusions, with a size range of 80–500 μm , are highly irregular and loose assemblages of concentrically zoned objects. Fine-grained spinel and needle-shaped phyllosilicates often occurs in the cores and Ca-pyroxene clusters near the periphery. Spinel-pyroxene inclusions have a relatively small size ranging from 70 μm to 240 μm . The three large inclusions are assemblages of several concentrically zoned objects that have spinel cores and Ca-pyroxene rims, and the smallest inclusion is a single concentric objects. Only one spinel spherule with a thin strongly altered rim was found in GRV 020025 (Figure 2C). It is 80 μm in diameter and a few small grains of perovskite are enclosed in spinel near the rim.

Spinel and Ca-pyroxene are the most common mineral components in the CAIs. Spinel generally contains less FeO (0.23–1.24%), TiO₂ (0.15–0.49%) and Cr₂O₃ (0.17–2.78%), although there is a small systematic change between type-A like inclusions (mean values of 0.70%, 0.85% and 1.66% for FeO, TiO₂ and Cr₂O₃, respectively) and spinel-pyroxene inclusions (mean values of 0.37%, 0.25% and 0.29% for FeO, TiO₂ and Cr₂O₃, respectively) in these minor element abundances. Similar to the spinel-pyroxene inclusions, spinel in spinel spherule contains lower FeO, TiO₂ and Cr₂O₃ (mean values of 0.38%, 0.30% and 0.14%, respectively). The content of TiO₂ is relatively low (<0.95%) in Ca-pyroxene of type-A-like inclusions and spinel-pyroxene inclusions. There is no obvious deviation in TiO₂, Al₂O₃, and FeO contents between these two types of CAIs. Phyllosilicates are also commonly present in all CAIs in GRV 020025 with low total oxides (80–86%).

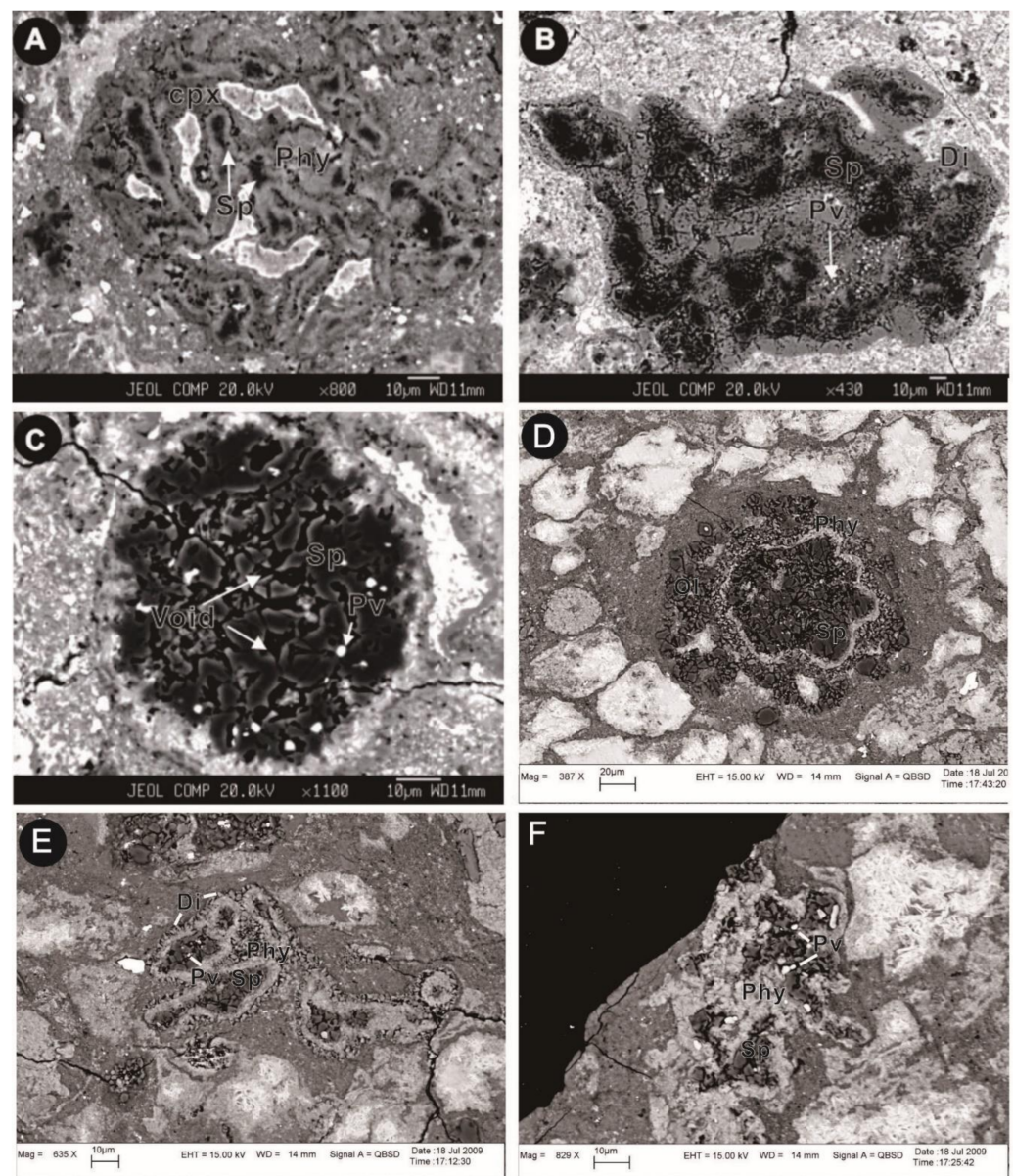


Figure 2. Backscattered electron images of refractory inclusions in GRV 020025 and GRV 050179; (A–C) reproduced from reference [13]: (A,B) type A-like inclusions; c: spinel spherule. (C–F) type A-like inclusions. Sp: spinel; Di: diopside; Ol: olivine; Pv: perovskite; Phyl: phyllosilicate; cpx: clinopyroxene.

3.3.2. GRV 050179

GRV 050179 has similar petrological characteristics to GRV 020025 in morphology, texture, mineral (or chondrule, matrix and CAIs), diameter, abundance and mineral assemblage (Table 2). Four type-A-like CAIs (one inclusion with forsterite-rich accretionary rim, Figure 2D–F) were found and experienced heavy alteration, which was indicated by the presence of abundant phyllosilicates. They have a size range from 50 μm to 400 μm . Most of these CAIs are irregularly shaped and loose assemblages of concentrically zoned objects, each of which consists of a core of fine-grained spinel and needle-shaped phyllosilicates and rims of Ca-pyroxene [18].

The spinel grains in GRV 050179 are FeO-poor (<1.04 wt%) and show similar compositions to those in GRV 020025 type-A inclusions in average FeO, TiO₂ and Cr₂O₃ contents (0.65, 0.84 and 1.61%, respectively). One analysis on Ca-pyroxene shows pyroxene has low contents of TiO₂ (1.19%), FeO (2.25%) and Cr₂O₃ (0.12%). Quantitative analyses on phyl-

losilicates show the commonly high FeO (23.6–40.5%) and the low total oxides (79–85%), which are suggestive of the presence of OH and/or H₂O [18].

4. Discussion

4.1. Petrologic Type and Chemical Group

4.1.1. GRV 020005

Previous studies have suggested that the petrologic types of these GRV CM chondrites are all type 2 (Table 1) [9]. Based on the above study of meteorite matrix (see the texts in Section 3.2), it is considered that the petrologic characteristics of GRV 020005 are similar to the type 1 meteorite of MET 01,070 [23]. Thus, the petrologic type of GRV 020005 should be reclassified as type 1 mainly for the following reasons [11]: (1) No anhydrous minerals (olivine and pyroxene) were found in the matrix and chondrule; (2) No metal in the matrix and chondrule; (3) The sulfide is mainly composed of pentlandite and a small amount of pyrrhotite and basically does not contain troilite; (4) Dolomite, a most heavily altered mineral in CCs [8,21], commonly appeared in this meteorite.

4.1.2. GRV 021579

According to the chondrule diameter (30–100 µm) and matrix/chondrule ratio (1.2, see Table 2), Dai et al. [18] first thought that GRV 021579 was a carbonaceous chondrite of type CO3, although the chondrule diameter had two peak ranges (350–600 µm and 30–100 µm). Later, Miao [13] studied another thin section from GRV 021579 and a similar matrix/chondrule ratio (1.1) was given. Soon after, Wang [11] studied a new section and found a high matrix abundance (78 vol%), which falls within the range of typical CM chondrites (50–80 vol%). The diameter of chondrules mostly falls in the range of 0.2–0.3 mm, which is also similar to the average chondrule diameter (0.3 mm) of CM chondrites. In addition, the minerals in the interstitial matrix have obviously undergone aqueous alteration and about one third of the matrix minerals has been altered into phyllosilicate. Therefore, they believe that the meteorite should be a CM2 meteorite [11].

4.2. Origin and Alteration of Matrix

According to the matrix whole rock composition (low total oxides), matrix mineralogy (olivine, pyroxene, magnetite, etc., as well as the coexistence of water-bearing minerals and anhydrous minerals), the composition difference (such as complementarity of Mg and Fe) and particle size difference between matrix and chondrule, Wang [11] believed that the interstitial matrix originates from nebular condensation. FGRs share similar characteristics in mineral composition and aqueous alteration with interstitial matrix. In addition, the morphological and structural characteristics of FGRs also show that FGRs are formed by gas–solid condensation and in the early Solar Nebula. Although the number of DIs is small (9 in total) and the research is weak, Wang [11] considered that DIs are very similar to the interstitial matrix, which may be formed by the condensation of interstellar dust material in the Solar Nebular prior to the parent body formation.

According to the study of the GRV CM matrix by Wang [11], the aqueous alteration of CCs is a multi-stage process. The meteorites first experienced pre-accretion aqueous alteration in the local environment of the nebula and then experienced a general aqueous alteration in the meteorite parent body. The evidence of alteration in the nebula environment is that the degree of alteration of chondrule is much lower than that of matrix. The matrix in GRV 020017 consists of different regions with varying degrees of alteration. This aqueous alteration probably occurred in the nebula condensation process rather than parent body. The records of altered minerals both in chondrule and in matrix, the fractionation of Ca and Al in matrix, and the occurrence of pentlandite and pyrrhotite show that this kind of alteration was commonly present in the parent body environment [11].

4.3. CAIs

4.3.1. Formation of CAIs

Most CAIs in the GRV CM chondrites are likely assemblages formed by Solar Nebular gas–solid condensates. The type-A-like inclusions are similar to fluffy type A (or referred as melilite-spinel-rich) inclusions that were extensively studied in Allende, Ningqiang, Murchison and GRV CCs [12,14,18,24–26]. They have the same characteristics of fluffy accretion of concentrically zoned objects, mineral assemblages and mineral chemistry with an assumption that melilite has been altered. CAIs have undergone extensive aqueous alteration indicated by the common presence of phyllosilicate. The results show that some CAIs cannot be clearly defined as type A-like or spinel-pyroxene-rich inclusions (Figure 2, also see Figures 5 and 6 in [14], Figure 2C,F in [18]). In fact, these two types of CAIs show a continuous trend of variation in modal composition by previous observation [25]. The chemical compositions of spinel and Ca-pyroxenes are undistinguished between the two type CAIs [14,18]. Mineral sequence of perovskite, melilite, spinel, Ca-pyroxene and forsterite from core to rim (Figure 2) is also consistent with the prediction of Solar Nebular condensation. Forsterite and/or Ca-pyroxene rims (Figure 2B,D,E), identical to Wark–Lovering rims [27], were formed by accretion of high-temperature condensates in the CAI-forming regions [28]. Several CAIs have more refractory rim of spinel, hibonite and perovskite supporting a high temperature evaporating process which probably occurred (Figure 2B,D,E). Crystallization from melts also cannot be excluded for the presence of spinel spherule and fragments with a few small grains of perovskite (Figure 2A,C,F, also see Figure 2C in [14]).

4.3.2. Alteration of CAIs

Almost all the CAIs in the GRV 020025 and GRV 050179 are heavily aqueously altered and indicated by the presence of abundant fine grains of secondary minerals (phyllosilicates). There is no melilite found in the CAIs of these two chondrites although melilite is referred to as a common component in the main types of CAIs. As a result, the fine-grained phyllosilicate is probably the alteration product of melilite by gas–solid or liquid–solid reaction. Ca-pyroxene and spinel are much more resistant to alteration, hence remained as the major mineral in CAIs.

Where and when the alteration took place is a controversial issue. However, it is certain that alteration is unlikely to occur on Earth after the falling of meteorites. Alteration products and spinel FeO contents in CAIs differ among meteorites and such a systematic difference does not seem to be caused by terrestrial weathering [18]. In addition, the alteration characteristics in CAIs of GRV CM chondrites are very similar to those in the fresh falling CM chondrite of Murchison [12]. The significant extinct radionuclide ^{36}Cl (half-life of 0.3 Ma) in sodalite in alteration assemblages of a Ningqiang CAI [29] and very high heterogeneity of CAI alteration in some CCs [28] favor the viewpoint of nebular alteration. $^{55}\text{Mn}/^{52}\text{Cr}$ ratio measurements give alteration ages between 2.3 and 8.0 Ma with an average value of 5.1 Ma after CAIs' formation [30], which match the peak heating time expected from the decay of short-lived ^{26}Al radioisotopes, implying that the primary driver of aqueous alteration was radiogenic decay [31]. Hence, a view of asteroidal alteration are more convincing. The widespread phyllosilicates in CAIs, chondrules and matrix in GRV CM chondrites also suggest aqueous alteration probably occurred in the parent body [12,18].

4.3.3. Type Distribution Patterns of CAIs

A number of previous studies show that the hibonite \pm spinel-rich and spinel \pm pyroxene-rich inclusions as well as AOAs are commonly preserved in the CMs while the melilite-rich and pyroxene-hibonite spherules are rare [19,28]. The survey of CAIs in the GRV CM chondrites and in the Allende and Murchison CCs, together with other GRV CCs [12,18,26], demonstrates that type A-like and spinel-pyroxene inclusions are the two dominant petrographic types and AOAs are also commonly present (Table 4). Although

there are some uncertainties in the relative abundances of various petrographic types of CAIs among meteorites, type A-like and spinel-pyroxene inclusions are much more abundant than the other types and such a difference cannot be attributed to statistical errors [12,26].

Table 4. Summary and comparison of Ca, Al-rich refractory inclusions and AOAs in GRV chondrites.

Groups	CM2				CV3		CO3
	Murchison	GRV 050179	GRV 020025 *	Allende	GRV 023155	GRV 022459	GRV 021579
Section number	2	1	1	4	1	1	1
Total areas (mm ²)	210	131	120	1090	108	29	62
Type A-like	9	4	12	40	4	3	4
Sp-Px/fragment	7		16	20			8
Hib-rich			2	1			
Sp Spherule/fragment	1		2	1			1
AOA			6	5		1	
Total	17	4	38	67	4	4	13

Data from [18]; *: Data from [12,20].

Only two hibonite-rich inclusions are present in GRV 020025 and one in Murchison (Table 4), although hibonite is one of the earliest condensates and its typical blue color makes hibonite easy to be recognized as well as become the most intensely studied CAIs in CM chondrites [19,28,32,33]. In previous studies, many spinel-hibonite spherules were separated from CM chondrites by freeze-saw method and density separation [19,28,32,33], hence, they are not representative of CAIs in these chondrites. The survey of two sections of Murchison reveals all of the CAIs are type A-like and spinel-pyroxene except for one section of euhedral spinel grains enclosed in coarse-grained Ca pyroxene [32]. Most of the 66 spinel-rich inclusions in Mighei chondrite (CM2) were recognized as spinel-pyroxene [34] and many of the others are similar to type A-like if the fine-grained assemblages are alteration products of melilite.

4.4. P-Bearing Sulfide Phase

So far, P has never been detected in terrestrial and extraterrestrial sulfides. Thus, P-bearing sulfide phase is an interesting component commonly present in the CM chondrites [17,35–37]. Some occurrences with flat and smooth surface and stoichiometric composition [36] indicate the P-bearing sulfide probably is a single mineral. However, the transmission electron microscopy of several P-bearing sulfide grains [35] showed that these grains probably consist of two unknown phases. As discussed in the Section 3 above, P-bearing sulfides were found in GRV CM chondrites and Zhang et al. [17] reported the occurrence, chemistry and oxygen isotopic compositions of P-bearing sulfide in GRV 021536 and Murchison. Limited variations in both chemical compositions and electron-diffraction patterns imply that the P-O-rich sulfide may be a single phase rather than a polyphase mixture. Previous study on the origins of P-bearing sulfide included condensation genesis [35], the sulfidization of an extrasolar precursor phase prior to condensation of FeNi metal [36] and an accessory product concurrent to the tochilinite formation during aqueous alteration of kamacite on the parent body [37]. According to the researches on GRV 021536 and Murchison, Zhang et al. believed that P-bearing sulfide formed during the sulfur-rich aqueous alteration of P-rich FeNi metal (first stage) before the carbonate (second stage) and tochilinite (third stage) formation on the parent body of CM chondrites [17].

5. Summary and Outlook

In general, the research progress of GRV meteorites mainly includes the following contents: (1) These meteorites have typical characteristics of CM chondrites indicated by the petrology, mineralogy and compositions. (2) These meteorites generally underwent varying degrees of aqueous alteration. The typical altered minerals (such as phyllosilicates,

pentlandite, pyrrhotite, troilite, calcite, etc.) commonly appeared and GRV 020005 is the most heavily altered of chondrites in GRV CMs with petrological type of 1. (3) A large number of CAIs and AOAs were discovered in GRV 020025. The main petrographic types of CAIs are type A-like and spinel-pyroxene inclusions. The minor are hibonite-rich inclusions and spinel spherules/fragments. There is no melilite found in the CAIs and the presence of abundant fine grains of phyllosilicates likely indicated heavily aqueous alteration. (4) P-bearing sulfides are present in the GRV CM chondrites.

Although some progresses have been made in the study of GRV CM chondrites, there are still three meteorites (GRV 021580, GRV 050384 and GRV 13051) that have not been studied or reported except on the Meteoritical Bulletin. This situation needs attention and more people need to participate in the research on these most primitive meteorites. More in-depth studies, such as the subclassification of GRV CM chondrites, the procession of aqueous alteration, conditions and timescales of alteration, the type distribution patterns of CAIs (and AOAs) and the P-bearing sulfide and so on, have not been well solved in previous studies. The nondestructive and high-resolution analysis on stable isotopes (oxygen, carbon, sulfur, nitrogen, etc.), short-lived radioactive nuclides (Al-Mg, Mn-Cr, Cl-S, etc.), presolar grains, etc., should also be applied in the future GRV CM researches to illuminate the nebula condensation process and parent body history.

Author Contributions: W.S.: Funding acquisition, writing, review and supervision; Z.L. and T.Z.: Table preparation and editing; M.Z. and J.G.: Figure preparation and editing; Z.Y. and W.H.: Review and editing. All authors have read and agreed to the published version of the manuscript.

Funding: This research was funded by the Science and Technology Program of Guangzhou, grant numbers 202002030184 and 201804010190, the Guangdong Natural Science Foundation, grant number 2021A1515011658 and the National Natural Science Foundation of China, grant numbers 42072229 and U1911202.

Acknowledgments: The authors thank all those who have contributed to GRV meteorite researches. Special thanks to D.D., X.W., B.M., Y.L. and A.Z.; we have quoted and commented on their fruitful research results. We are also grateful to G.W. for inviting us to write this article.

Conflicts of Interest: The authors declare no conflict of interest.

References

1. Halliday, A.N. 2.8—The origin and earliest history of the Earth. In *Treatise on Geochemistry*, 2nd ed.; Holland, H.D., Turekian, K.K., Eds.; Elsevier: Oxford, UK, 2014; pp. 149–211.
2. Gilmour, I. 1.5—Structural and isotopic analysis of organic matter in carbonaceous chondrites. In *Treatise on Geochemistry*, 2nd ed.; Holland, H.D., Turekian, K.K., Eds.; Elsevier: Oxford, UK, 2014; pp. 215–233.
3. Martins, Z.; Chan, Q.H.S.; Bonal, L.; King, A.; Yabuta, H. Organic matter in the Solar System—Implications for future on-site and sample return missions. *Space Sci. Rev.* **2020**, *216*, 54. [[CrossRef](#)]
4. Weisberg, M.K.; McCoy, T.J.; Krot, A.N.; Binzel, R.P.; Walker, R.M.; Cameron, A.G.W. Systematics and evaluation of meteorite classification. In *Meteorites and the Early Solar System II*; Lauretta, D.S., McSween, H.Y., Eds.; University of Arizona Press: Tucson, AZ, USA, 2006; pp. 19–52.
5. Metzler, K.; Hezel, D.C.; Barosch, J.; Wölfer, E.; Schneider, J.M.; Hellmann, J.L.; Berndt, J.; Stracke, A.; Gattacceca, J.; Greenwood, R.C.; et al. The Loongana (CL) group of carbonaceous chondrites. *Geochim. Cosmochim. Acta* **2021**, *304*, 1–31. [[CrossRef](#)]
6. Zolensky, M.E.; Weisberg, M.K.; Buchanan, P.C.; Mittlefehldt, D.W. Mineralogy of carbonaceous chondrite clasts in HED achondrites and the Moon. *Meteorit. Planet. Sci.* **1996**, *31*, 18–537. [[CrossRef](#)]
7. Lunning, N.G.; Corrigan, C.M.; McSween, H.Y.; Tenner, T.J.; Kita, N.T.; Bodnar, R.J. CV and CM chondrite impact melts. *Geochim. Cosmochim. Acta* **2016**, *189*, 38–358. [[CrossRef](#)]
8. Zolensky, M.E.; Mittlefehldt, D.W.; Lipschutz, M.E.; Wang, M.-S.; Clayton, R.N.; Mayeda, T.K.; Grady, M.M.; Pillinger, C.; David, B. CM chondrites exhibit the complete petrologic range from type 2 to 1. *Geochim. Cosmochim. Acta* **1997**, *61*, 5099–5115. [[CrossRef](#)]
9. Meteoritical Bulletin: Search for the Meteoritical Bulletin Database. Available online: <https://www.lpi.usra.edu/meteor/> (accessed on 1 February 2022).
10. Miao, B.; Hu, S.; Chen, H.; Zhang, C.; Xia, Z.; Huang, L.; Xue, Y.; Xie, L. Progresses of researches on meteoritics and cosmochemistry from 2011 to 2020 in China. *Bull. Mineral. Petrol. Geochem.* **2021**, *40*, 1–15, (In Chinese with English abstract). [[CrossRef](#)]
11. Wang, X. Study on the Petrology and Origin of Matrix of Antarctic Carbonaceous Chondrites. Master's Thesis, Guilin University of Technology, Guilin, China, 2009. (In Chinese)

12. Dai, D. Classification of 104 Meteorites Collected in Grove Mountains, Antarctic, and a Comparative Study of Ca, Al-Rich Inclusions (CAIs) from Various Groups of Chondrites. Ph.D. Thesis, School of the Chinese Academy of Sciences, Guangzhou, China, 2007. (In Chinese)
13. Miao, B. Comprehensive Study of Meteorites from Grove Mountains, Antarctica. Postdoctoral Research Report; Institute of Geology and Geophysics, Chinese Academy of Sciences: Beijing, China, 2008. (In Chinese)
14. Dai, D.; Lin, Y.; Miao, B.; Shen, W.; Wang, D. Ca-, Al-rich inclusions in three new carbonaceous chondrites from the Grove Mountains, Antarctica: New evidence for a similar origin of the objects in various groups of chondrites. *Acta Geol. Sin.* **2004**, *78*, 1042–1051.
15. Dai, D.; Wang, D. Petrography and mineral chemistry of 4 carbonaceous chondrites from the Grove Mountains, Antarctica. *Chin. J. Polar Res.* **2009**, *20*, 166–171.
16. Dai, D.; Chen, X.; Yang, R. The study of and expectations for finding carbonaceous chondrites in the Grove Mountains, Antarctica. *Chin. J. Polar Res.* **2013**, *25*, 378–385. (In Chinese) [[CrossRef](#)]
17. Zhang, A.C.; Itoh, S.; Yurimoto, H.; Hsu, W.B.; Wang, R.C.; Taylor, L.A. P-O-rich sulfide phase in CM chondrites: Constraints on its origin on the CM parent body. *Meteorit. Planet. Sci.* **2016**, *51*, 56–69. [[CrossRef](#)]
18. Dai, D.; Zhou, C.; Chen, X. Ca-, Al-rich inclusions in two new carbonaceous chondrites from Grove Mountains, Antarctica. *Earth Moon Planets* **2015**, *115*, 101–114. [[CrossRef](#)]
19. Scott, E.R.D.; Krot, A.N. 1.2—Chondrites and their components. In *Treatise on Geochemistry*, 2nd ed.; Holland, H.D., Turekian, K.K., Eds.; Elsevier: Oxford, UK, 2014; pp. 65–137.
20. Shen, W.; Miao, B.; Lin, Y. A fine study on petrology and mineralogy of carbonaceous chondrite GRV 020025. In Proceedings of the 10th National Symposium on Lunar Science, Comparative Planetary, Meteorology and Cosmochemistry, Guilin, China, 24 October 2012; p. 45.
21. Rubin, A.E.; Trigo-Rodríguez, J.M.; Huber, H.; Wasson, J.T. Progressive aqueous alteration of CM carbonaceous chondrites. *Geochim. Cosmochim. Acta* **2007**, *71*, 2361–2382. [[CrossRef](#)]
22. Van Kooten, E.M.M.E.; Cavalcante, L.L.; Nagashima, K.; Kasama, T.; Balogh, Z.I.; Peeters, Z.; Hsiao, S.S.-Y.; Shang, H.; Lee, D.C.; Lee, T.; et al. Isotope record of mineralogical changes in a spectrum of aqueously altered CM chondrites. *Geochim. Cosmochim. Acta* **2018**, *237*, 9–102. [[CrossRef](#)]
23. Trigo-Rodríguez, J.M.; Rubin, A.E. Evidence for parent-body aqueous flow in the MET 01070 CM carbonaceous chondrite. *Lunar Planet. Sci.* **2006**, *XXXVII*, 104.
24. Macpherson, G.J.; Grossman, L. ‘Fluffy’ Type A Ca-, Al-rich inclusions in the Allende meteorite. *Geochim. Cosmochim. Acta* **1984**, *48*, 29–46. [[CrossRef](#)]
25. Lin, Y.; Kimura, M. Ca-Al-rich inclusions from the Ningqiang meteorite: Continuous assemblages of nebular condensates and genetic link to Type B inclusions. *Geochim. Cosmochim. Acta* **2003**, *67*, 251–2267. [[CrossRef](#)]
26. Lin, Y.; Kimura, M.; Miao, B.; Dai, D.; Monoi, A. Petrographic comparison of refractory inclusions from different chemical groups of chondrites. *Meteorit. Planet. Sci.* **2006**, *41*, 67–81. [[CrossRef](#)]
27. Wark, D.; Boynton, W.V. The formation of rims on calcium-aluminum-rich inclusions: Step I-Flash heating. *Meteorit. Planet. Sci.* **2001**, *36*, 1135–1166. [[CrossRef](#)]
28. MacPherson, G.J. 1.3—Calcium–aluminum-rich inclusions in chondritic meteorites. In *Treatise on Geochemistry*, 2nd ed.; Holland, H.D., Turekian, K.K., Eds.; Elsevier: Oxford, UK, 2014; pp. 139–179.
29. Lin, Y.; Guan, Y.; Leshin, L.A.; Ouyang, Z.; Wang, D. Short-lived chlorine-36 in a Ca- and Al-rich inclusion from the Ningqiang carbonaceous chondrite. *Proc. Natl. Acad. Sci. USA* **2005**, *102*, 306–1311. [[CrossRef](#)]
30. Suttle, M.D.; King, A.J.; Schofield, P.F.; Bates, H.; Russell, S.S. The aqueous alteration of CM chondrites, a review. *Geochim. Cosmochim. Acta* **2021**, *299*, 19–256. [[CrossRef](#)]
31. Doyle, P.M.; Jogo, K.; Nagashima, K.; Krot, A.N.; Wakita, S.; Ciesla, F.J.; Hutcheon, I.D. Early aqueous activity on the ordinary and carbonaceous chondrite parent bodies recorded by fayalite. *Nat. Commun.* **2015**, *6*, 7444. [[CrossRef](#)] [[PubMed](#)]
32. Liu, M.C.; Chaussidon, M.; Göpel, C.; Lee, T. A heterogeneous solar nebula as sampled by CM hibonite grains. *Earth Planet. Sci. Lett.* **2012**, *327–328*, 5–83. [[CrossRef](#)]
33. Liu, M.C.; McKeegan, K.D.; Goswami, J.N.; Marhas, K.K.; Sahijpal, S.; Ireland, T.R.; Davis, A.M. Isotopic records in CM hibonites: Implications for timescales of mixing of isotope reservoirs in the solar nebula. *Geochim. Cosmochim. Acta* **2009**, *73*, 5051–5079. [[CrossRef](#)]
34. MacPherson, G.J.; Davis, A.M. Refractory inclusions in the prototypical CM chondrite, Mighei. *Geochim. Cosmochim. Acta* **1994**, *58*, 5599–5625. [[CrossRef](#)]
35. Devouard, B.; Buseck, P.R. Phosphorous-rich iron, nickel sulfides in CM2 chondrites: Condensation or alteration products? *Meteoritics* **1997**, *32*, A34.
36. Nazarov, M.A.; Kurat, G.; Brandstaetter, F.; Ntaflou, T.; Hoppe, P. Phosphorus-bearing sulfides and their associations in CM chondrites. *Petrology* **2009**, *17*, 101–123. [[CrossRef](#)]
37. Palmer, E.E.; Lauretta, D.S. Aqueous alteration of kamacite in CM chondrites. *Meteorit. Planet. Sci.* **2011**, *46*, 1587–1607. [[CrossRef](#)]